# Adiabatic-following criterion, estimation of the nonadiabatic excitation fraction, and quantum jumps

R. N. Shakhmuratov[1,2] and J. Odeurs[1]
[1]*Instituut voor Kern- en Stralingsfysica, Katholieke Universiteit Leuven, Celestijnenlaan 200 D, B-3001 Leuven, Belgium*
[2]*Kazan Physical-Technical Institute, Russian Academy of Sciences, 10/7 Sibirsky Trakt Street, Kazan 420029, Russia*
(Received 28 October 2002; revised manuscript received 26 February 2003; published 6 October 2003)

An accurate theory describing adiabatic following of the dark, nonabsorbing state in the three-level system is developed. An analytical solution for the wave function of the particle experiencing Raman excitation is found as an expansion in terms of the time varying nonadiabatic perturbation parameter. The solution can be presented as a sum of adiabatic and nonadiabatic parts. Both are estimated quantitatively. It is shown that the limiting value to which the amplitude of the nonadiabatic part tends is equal to the Fourier component of the nonadiabatic perturbation parameter taken at the Rabi frequency of the Raman excitation. The time scale of the variation of both parts is found. While the adiabatic part of the solution varies slowly and follows the change of the nonadiabatic perturbation parameter, the nonadiabatic part appears almost instantly, revealing a jumpwise transition between the dark and bright states. This jump happens when the nonadiabatic perturbation parameter takes its maximum value.

DOI: 10.1103/PhysRevA.68.043802 PACS number(s): 42.50.Gy, 32.80.Qk, 42.50.Md, 42.50.Hz

## I. INTRODUCTION

Stimulated Raman adiabatic passage (STIRAP) resulting in the population transfer between the states which are not directly coupled [1], electromagnetically induced transparency via adiabatic following of the dark, nonabsorbing state [2], nonresonant pulse excitation of the two-level atom [3] are just a short list of phenomena in quantum optics where adiabatic processes are considered. Generally, one can find in any part of physics problems concerned with adiabaticity, which are treated almost similarly. Among them we can mention multiphoton resonances induced in atoms and molecules by a strong low-frequency field [4–7], wave-packet dynamics in physics and chemistry or, so-called, ''femtochemistry'' [8–10], and slow atomic and molecular collisions [11–18].

In this paper we consider the adiabatic following of the dark, nonabsorbing state in the three-level system, excited by two resonant fields, which results in STIRAP (population transfer). It was proposed in Ref. [19] where the so-called counterintuitive Raman pulse sequence emerged as a result of the search for the generalization of the Liouville equations for the $N$-level system using SU($N$) coherence vector theory [20,21]. This pulse sequence consists of two fields coupling two low-energy levels 1 and 2 with one common excited state 3. If one of the levels (for example, 2) is initially empty, then applying first the field which couples this state with level 3, and then the field coupling the populated state (for example, 1) with 3, it is possible to transfer the population of state 1 to state 2, without appreciably populating the intermediate state 3.

Later, the importance of the adiabaticity in the counterintuitive pulse sequence development was realized in Refs. [22–24]. There is a particular superposition of states 1 and 2 that does not interact with the coupling fields and, if the development of the field amplitudes in time is properly chosen, this superposition state changes from state 1 to state 2. If the three-level atom follows this superposition state, the atom population is transferred from state 1 to state 2 by the pulse sequence without populating the intermediate excited state 3. This noncoupled superposition state was first introduced by Arimondo [25] to explain qualitatively the dark resonance as population trapping in this state [26–28]. The noncoupled state is often referred to as a dark state.

It is obvious that, if the dark state changes in time, a process must exist which tends to empty this state. The condition minimizing the dark state depopulation is formulated in Ref. [22]. This is done *ad hoc*, without an estimation of the nonadiabatic correction for the excited probability amplitude. However, numerical calculations show that, if this condition is satisfied, the adiabatic population transfer $1\rightarrow 2$ is almost perfect. Some attempts were undertaken to find a rigorous justification of the intuitively found adiabaticity condition and to estimate the amplitude of the excited state during the STIRAP pulse sequence (see, for example, Refs. [29,30]). In Ref. [29], the so-called ramp pulses were considered, which allow an exact solution. Furthermore, with the help of the method developed for the two-level system by Dykhne (see Refs. [31,32] and the discussion in Refs. [33,34]), the nonadiabatic amplitude of the excited state 3 is estimated for Gaussian and hyperbolic secant pulses. This is possible because the Liouville equation for the two-level atom in terms of the SU(2) coherence vector (Bloch-vector model) coincides with the Schrödinger equation for the state probability amplitudes of the three-level atom excited by two resonant fields (see, for example, Refs. [2,24,29]). However, the authors of Ref. [29] admit that the analytical approximations for the nonadiabatic corrections ''*have been introduced ad hoc without derivation*'' and they ''*would really like to see more detailed investigations of the analytic behavior of the system discussed*.''

Fleischhauer and co-workers [30] developed a different approach introducing higher-order trapping states. They define an $n$th-order generalized adiabatic basis, which is similar to the superadiabatic basis introduced for the two-level system in Refs. [35–38]. By successive transformations from

 

the diabatic basis to the adiabatic basis, then from this adiabatic basis, which can be considered as the adiabatic basis of the first order, to the next, i.e., the second-order adiabatic basis, etc., the solution is presented as an infinite product of transformations. The general expression for the $n$th transformation matrix is presented. However, it is hard to implement this scheme for an arbitrary pulse sequence.

In this paper we develop a method that allows us to calculate the adiabatic and nonadiabatic components of the solution with controllable accuracy. The adiabatic component describes the part of the atomic probability amplitude visiting the excited atomic state during the pulse train and coming back to the dark state when the pulses are gone. The atom evolution following the adiabatic component of the solution resembles the excitation-deexcitation process induced by a soliton in the two-level atom. The nonadiabatic component is that part which is lost from the dark state and describes the fraction of the atomic probability amplitude that is left excited after the pulse train. We compare our result with the previous theories reported in Refs. [29,30]. We found corrections to the theory presented in Ref. [29] and show that our result corresponds to the calculation of the infinite number of transformations proposed in Ref. [30].

The paper is organized as follows. In Sec. II we present the general formalism employed in the description of the three-level atom excited by two resonant fields. The transformation to the basis of the bright and dark states is derived. It is shown that the system evolves between two states, i.e., ''bright'' and ''common'' (they are specified in Sec. II). In Sec. III we consider the time evolution of the atomic state vector for the $\Lambda$ scheme of excitation if the field amplitudes are time dependent. Bloch-like equations are derived. In Sec. IV the adiabatic-following approximation is presented. The adiabatic solution for the STIRAP is found. Nonadiabatic corrections are described in Sec. V. The case when the Raman Rabi frequency changes in time is considered in Sec. VI–VIII.

## II. THREE-LEVEL ATOM INTERACTING WITH TWO RESONANT FIELDS: GENERAL FORMALISM

We consider a three-level atom shown in Fig. 1(a). The arrows indicate the transitions induced by the coherent fields. We define the level that is common for both transitions as 3. The others are designated by the numbers 1 and 2, level 2 being of higher energy than 1 and initially not populated. The dynamic part of the Hamiltonian of this three-level atom, excited by two resonant fields $\mathbf{E}_1(t)=\mathbf{E}_1\cos(\Omega_1 t+\varphi_1)$ and $\mathbf{E}_2(t)=\mathbf{E}_2\cos(\Omega_2 t+\varphi_2)$, is

$$H=\sum_{n=1}^{3}\omega_n\hat{P}_{nn}-(B_1\hat{P}_{13}e^{i\Omega_1 t+i\varphi_1}+B_2\hat{P}_{23}e^{i\Omega_2 t+i\varphi_2}+\text{H.c.}), \tag{1}$$

where $\omega_n$ is the energy of the state $n$. Planck's constant is set equal to 1 ($\hbar=1$) for simplicity. The operators $\hat{P}_{mn}$ are defined by $\hat{P}_{mn}=|m\rangle\langle n|$, where $\langle n|$ and $|m\rangle$ are bra and ket vectors of the states $n$ and $m$ in the Schrödinger representation. The interaction constant (Rabi frequency) $B_n=(\mathbf{d}_{n3}\cdot\mathbf{E}_n)/2=(\mathbf{d}_{3n}\cdot\mathbf{E}_n)/2$ depends on the dipole-transition matrix element, taken real so, $\mathbf{d}_{n3}=\mathbf{d}_{3n}$, and on the field amplitude $\mathbf{E}_n$. The rotating wave approximation is taken into account.

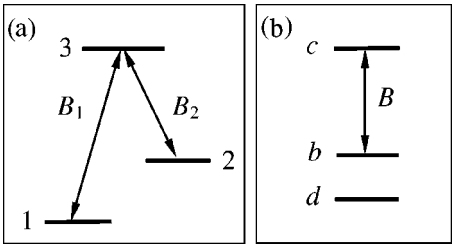


FIG. 1. The excitation scheme of the three-level atom by two resonant fields with interaction constants $B_1$ and $B_2$: $\Lambda$ scheme (a), and the same excitation scheme in the basis of dark $d$, bright $b$, and common $c$ states (b). $B=\sqrt{B_1^2+B_2^2}$ is the generalized interaction constant for the Raman excitation. The vertical scale in diagram (b) is not the energy and represents the initial population of the levels before the excitation. The higher populated level is put at the bottom and the lower or unpopulated level is at the top.

If the fields $\mathbf{E}_1(t)$ and $\mathbf{E}_2(t)$ are in exact resonance with the relevant transitions, the Hamiltonian, Eq. (1), can be made slowly varying by transforming it into the interaction representation (IR). This representation is defined by a canonical transformation by means of the unitary operator

$$T=\exp\left(i\sum_{n=1}^{3}\omega_n\hat{P}_{nn}t\right). \tag{2}$$

The wave function of the atom in the IR is defined by $|\Phi(t)\rangle=T|\Psi(t)\rangle$, where $|\Psi(t)\rangle$ is the wave function in the Schrödinger representation. $|\Phi(t)\rangle$ satisfies the Schrödinger equation with the effective Hamiltonian

$$\mathcal{H}=THT^{-1}+i\dot{T}T^{-1}. \tag{3}$$

This Hamiltonian has the explicit form

$$\mathcal{H}=-B_1\hat{P}_{13}e^{i\varphi_1}-B_2\hat{P}_{23}e^{i\varphi_2}+\text{H.c.}, \tag{4}$$

or in matrix notation

$$\mathcal{H}=-\begin{bmatrix}0 & 0 & B_1e^{i\varphi_1}\\ 0 & 0 & B_2e^{i\varphi_2}\\ B_1e^{-i\varphi_1} & B_2e^{-i\varphi_2} & 0\end{bmatrix}. \tag{5}$$

The $\hat{P}_{MN}$ operators are defined for the vectors $|M\rangle$ and $\langle N|$ of the interaction representation differing from the states $|m\rangle$ and $\langle n|$ by the phase factors $\exp(-i\omega_m t)$ and $\exp(i\omega_n t)$.

Assume that the field amplitudes $B_1$, $B_2$ and the phases $\varphi_1$, $\varphi_2$ are constant. Then the Hamiltonian, Eqs. (4)–(5), is diagonalized by a unitary transformation

$$\bar{\mathcal{H}}=Q\mathcal{H}Q^{-1}=\sqrt{B_1^2+B_2^2}(\hat{P}_{\overline{33}}-\hat{P}_{\overline{11}}), \tag{6}$$

where

$$Q=\frac{1}{\sqrt{2}}\begin{bmatrix} e^{-i\varphi_1}\sin\alpha & e^{-i\varphi_2}\cos\alpha & 1 \\ \sqrt{2}e^{i\varphi_2}\cos\alpha & -\sqrt{2}e^{i\varphi_1}\sin\alpha & 0 \\ e^{-i\varphi_1}\sin\alpha & e^{-i\varphi_2}\cos\alpha & -1 \end{bmatrix} \tag{7}$$

and $\tan\alpha=B_1/B_2$. The new ket vectors $|\overline{n}\rangle$ are related to the former ones $|N\rangle$, defined in the interaction representation, as follows $|\overline{\Phi}\rangle=Q|\Phi\rangle$. The explicit relations are

$$|\overline{1}\rangle=\frac{\sqrt{2}}{2}(e^{i\varphi_1}\sin\alpha|1\rangle+e^{i\varphi_2}\cos\alpha|2\rangle+|3\rangle), \tag{8}$$

$$|\overline{2}\rangle=e^{-i\varphi_2}\cos\alpha|1\rangle-e^{-i\varphi_1}\sin\alpha|2\rangle, \tag{9}$$

$$|\overline{3}\rangle=\frac{\sqrt{2}}{2}(e^{i\varphi_1}\sin\alpha|1\rangle+e^{i\varphi_2}\cos\alpha|2\rangle-|3\rangle). \tag{10}$$

The basis $|\overline{n}\rangle$, in which the Hamiltonian is diagonal, is called the basis of the quasienergy states [39,40]. It coincides with the basis of the dressed states if the limit of the classical field is taken for them.

States $|\overline{1}\rangle$ and $|\overline{3}\rangle$ are mixtures of all unperturbed states $|1\rangle$, $|2\rangle$, and $|3\rangle$, whereas state $|\overline{2}\rangle$ does not contain the common state $|3\rangle$. If the atom is in state $|\overline{2}\rangle$, a mixture of the ground-state sublevels 1 and 2, the atom does not leave this state since it is an eigenstate of the interaction Hamiltonian, Eq. (6). The bichromatic field $\mathbf{E}(t)=\mathbf{E}_1(t)+\mathbf{E}_2(t)$ does not interact with such an atom, and, consequently, it is not excited. Therefore, we call this state a dark state and designate it $|d\rangle$. This state was introduced for the first time by Arimondo in Ref. [25], who called this state a noncoupled state. He introduced the coupled state as well, which interacts with the bichromatic field $\mathbf{E}(t)$. Following Arimondo we define the state

$$|b\rangle=e^{i\varphi_1}\sin\alpha|1\rangle+e^{i\varphi_2}\cos\alpha|2\rangle, \tag{11}$$

which is orthogonal to the dark state. We call this state a bright state, since for the $\Lambda$ scheme, if the atom is in this state, it is excited by the bichromatic field and then the luminescence from state $|3\rangle$ may follow. Excitation can take place because the bright state is not an eigenstate of the interaction Hamiltonian, Eq. (6).

The states $|d\rangle$, $|b\rangle$, and $|3\rangle$ are mutually orthogonal and can be chosen as a new basis. We call this basis $dbc$, designating the state $|3\rangle$ by the letter $|c\rangle$, since it is common for the induced transitions. Because we will often refer to these states, they are presented below in a common set of equations to simplify further citation:

$$|d\rangle=e^{-i\varphi_2}\cos\alpha|1\rangle-e^{-i\varphi_1}\sin\alpha|2\rangle, \tag{12}$$

$$|b\rangle=e^{i\varphi_1}\sin\alpha|1\rangle+e^{i\varphi_2}\cos\alpha|2\rangle, \tag{13}$$

$$|c\rangle=|3\rangle. \tag{14}$$

The interaction Hamiltonian, Eqs. (4) and (5), is transformed in this basis as follows:

$$\mathcal{H}_{dbc}=S\mathcal{H}S^{-1}=-B(\hat{P}_{bc}+\hat{P}_{cb}), \tag{15}$$

or in a matrix form

$$\mathcal{H}_{dbc}=-\begin{bmatrix} 0 & 0 & 0 \\ 0 & 0 & B \\ 0 & B & 0 \end{bmatrix}, \tag{16}$$

where $B=\sqrt{B_1^2+B_2^2}$ and the unitary operator of the canonical transformation is

$$S=\begin{bmatrix} e^{i\varphi_2}\cos\alpha & -e^{i\varphi_1}\sin\alpha & 0 \\ e^{-i\varphi_1}\sin\alpha & e^{-i\varphi_2}\cos\alpha & 0 \\ 0 & 0 & 1 \end{bmatrix}. \tag{17}$$

We call this basis the $dbc$ representation.

Figure 1(b) shows the excitation scheme in the $dbc$ basis where only the $b$ and $c$ states are coupled. The $b$ and $c$ states do not correspond to a defined energy. To present schematically the $dbc$ states and the transitions between them, we choose the state population before the excitation for their relative position in the diagram. So, the vertical scale in Fig. 1(b) represents the initial population of the states counted from the bottom to the top.

The Hamiltonian in the $dbc$ basis, Eq. (15), resembles the interaction Hamiltonian of the two-level system $bc$, excited by one resonant field with an effective interaction constant $B$. The dynamic evolution of the atom is described by the Schrödinger equation with this Hamiltonian containing only the transition operators between states $b$ and $c$.

## III. TIME-DEPENDENT AMPLITUDES

If during the pulse excitation the field amplitudes $\mathbf{E}_1$, $\mathbf{E}_2$ are time dependent and they have the same time evolution satisfying the condition $B_1(t)/B_2(t)=\tan\alpha=\text{const}$, then the developments of the $|d\rangle$, $|b\rangle$ states in the ket vectors $|1\rangle$, $|2\rangle$ have constant coefficients and the $S$ transformation is time independent. In this case the solution of the Schrödinger equation is simple and the development coefficients of the state vector $|\Phi_{dbc}\rangle$,

$$|\Phi_{dbc}(t)\rangle=C_d(t)|d\rangle+C_b(t)|b\rangle+C_c(t)|c\rangle, \tag{18}$$

are $C_d(t)=C_d(0)$, $C_b(t)=C_b(0)\cos[\theta(t)/2]$, and $C_c(t)=iC_b(0)\sin[\theta(t)/2]$, where $C_d(0)$, $C_b(0)$ are the initial values of the probability amplitudes and $\theta(t)=2\int_{-\infty}^{t}B(\tau)d\tau$ is the pulse area of the bichromatic field. This case corresponds to so-called matched pulses [41,42].

If there is a time shift $T$ between the pulses $\mathbf{E}_1(t)$ and $\mathbf{E}_2(t)$, one can again introduce the bright and dark states, employing the time-dependent $S$ transformation. Then the evolution of the state vector of the atom in the $dbc$ basis is given by

$$|\Phi_{dbc}(t)\rangle=S(t)|\Phi(t)\rangle, \tag{19}$$

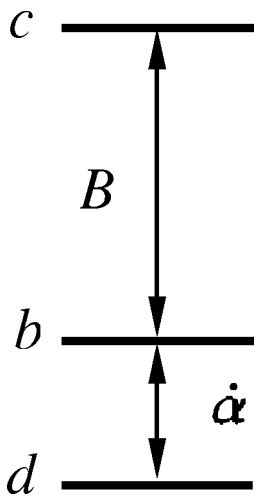


FIG. 2. The bichromatic excitation scheme of the three-level atom in the $dbc$ basis if the state developments of $|d\rangle$ and $|b\rangle$ change in time. The coupling parameter of states $d$ and $b$ is $\dot{\alpha}$, the derivative of the mixing angle (see the text).

where $|\Phi(t)\rangle$ is the state vector in the interaction representation. Taking the time derivative of Eq. (19), one can obtain the Schrödinger equation

$$\frac{d|\Phi_{dbc}\rangle}{dt} = -i\overline{\mathcal{H}}_{dbc}|\Phi_{dbc}\rangle \tag{20}$$

with the modified Hamiltonian

$$\overline{\mathcal{H}}_{dbc} = \mathcal{H}_{dbc} + i\dot{S}S^{-1}, \tag{21}$$

where $\mathcal{H}_{dbc}$ is defined in Eq. (15) and

$$i\dot{S}S^{-1} = i\dot{\alpha}[\hat{P}_{bd}e^{-i(\varphi_1+\varphi_2)} - \hat{P}_{db}e^{i(\varphi_1+\varphi_2)}]. \tag{22}$$

The first part $\mathcal{H}_{dbc}$ of the modified Hamiltonian induces transitions between the $|b\rangle$ and $|c\rangle$ states with the rate $\chi_R = 2B$, and the second part $i\dot{S}S^{-1}$, induces transitions between states $|d\rangle$ and $|b\rangle$ with the rate $2\dot{\alpha}$ (see Fig. 2).

The development coefficients of the state vector $|\Phi_{dbc}\rangle$ satisfy the equations

$$\dot{Z}_d = -\dot{\alpha}Y_b, \tag{23}$$

$$\dot{Y}_b = -BX_c + \dot{\alpha}Z_d, \tag{24}$$

$$\dot{X}_c = BY_b, \tag{25}$$

where the substitution $Z_d = C_d\exp(-i\varphi_2)$, $Y_b = C_b\exp(i\varphi_1)$, $X_c = -iC_c\exp(i\varphi_1)$ is made to deal with real numbers. Here the phases $\varphi_1$ and $\varphi_2$ are assumed to be constant throughout the excitation process. Equations (23)–(25) remarkably coincide with the Bloch equations for an abstract two-level system $g$-$e$ excited by a field with frequency $\omega$ slightly tuned from resonance ($g$ and $e$ being ground and excited states, respectively) [2]. Expressed in terms of the Bloch-vector components, which are the following combinations of the density matrix of the two-level system $\rho$: $u - iv = 2\rho_{ge}\exp(-i\omega t)$ and $w = \rho_{gg} - \rho_{ee}$, these equations are

$$\dot{w} = -\chi v, \tag{26}$$

$$\dot{v} = -\Delta u + \chi w, \tag{27}$$

$$\dot{u} = \Delta v. \tag{28}$$

Here $\Delta$ is the detuning from resonance and $\chi$ is the Rabi frequency. If one makes the substitution $w = Z_d$, $v = Y_b$, $u = X_c$ for the variables and $\chi = \dot{\alpha}$, $\Delta = B$ for the parameters, both sets of equations are identical.

The coincidence of the equations enables us to use the adiabatic-following approach developed by Crisp [3] to describe nonresonant excitation of the two-level system. A similar approach was applied by Laine and Stenholm (LS) [29] based on the ideas of the adiabatic following developed by Dykhne [31,32] for the two-level system with time-dependent splitting and coupling parameters. In the LS approach [29], the instantaneous eigenstates of the three-level atom excited by two resonant pulses are found. This basis is called the adiabatic representation. The transformation to the instantaneous basis [see Eq. (7)] and the instantaneous Hamiltonian diagonal in this basis [see Eq. (6)] are time dependent. Therefore, the adiabatic states coupling $i\dot{Q}Q^{-1}$ also appears in their consideration. In spite of being different in structure, our Schrödinger equation in the changing $dbc$ basis and the LS equation in the instantaneous eigenstate basis can both be reduced to the equation for the two-level system. However, our Eqs. (23)–(25) are in a one to one correspondence with the Bloch equations while the LS equations match the equations for the two-level density matrix elements $\rho_{eg}$, $\rho_{ge}$, and $\rho_{gg} - \rho_{ee}$. Although this difference is not crucial, it brings, however, some convenience in our case, because our equations are expressed for real quantities.

## IV. ADIABATIC SOLUTION

The adiabatic-following approximation can be applied to the consideration of STIRAP and electromagnetically induced transparency (EIT) because in both cases the atom follows the dark, noncoupled state. A first attempt to study adiabatic following in EIT was undertaken in Ref. [2]. In this section we consider the application of this approach to STIRAP.

The stimulated Raman adiabatic passage assumes that before the application of the $E_1(t)$ and $E_2(t)$ pulses the atom is in state $|1\rangle$. The duration of the excitation as well as the pulse sequence must be chosen such that at the end of the pulse train the atom is left in state $|2\rangle$. It is expected that during this process the atom stays in the dark state. However, this state itself changes since the coefficients $\cos\alpha$ and $\sin\alpha$ of the development of the dark state in the vectors $|1\rangle$ and $|2\rangle$ [see Eq. (12)] change in time. The parameter $\alpha$ rises from zero to $\pi/2$, so $|d\rangle = |1\rangle$ before the excitation and $|d\rangle = -e^{-i(\varphi_1-\varphi_2)}|2\rangle$ after it. Since $\tan\alpha = B_1/B_2$, the condition imposed on $\alpha$ means that the $B_1(t)$ pulse must be de-

layed with respect to the $B_2(t)$ pulse. We have to emphasize that the phase of the final state 2 after the pulse train is related to the phase of the initial state 1 according to Eq. (12).

If we choose two identical, bell-shaped, delayed pulses having a hyperbolic secant shape, then the interaction constants evolve in time as follows:

$$B_n(t) = B_0 \,\mathrm{sech}[r(t-t_n)], \tag{29}$$

where $n=1$ or 2, $t_n$ is the time when the $n$-pulse has maximum amplitude, and $r$ is the rise and fall rate of the pulse edges. The mixing parameter $\alpha(t)$ increases monotonously if the condition $t_1 > t_2$ is satisfied. This pulse sequence was considered by Laine and Stenholm in Ref. [29].

Let us analyze the constraints imposed on the parameters $r$, $t_1$, and $t_2$ to have $\alpha$ changed from zero to $\pi/2$. The mixing angle $\alpha$ varies according to the relation $\tan\alpha(t) = B_1(t)/B_2(t)$. For the pulse sequence specified above, an explicit form of this relation is

$$\tan\alpha(t) = \frac{1 + D\tanh[r(t-t_0)]}{1 - D\tanh[r(t-t_0)]}, \tag{30}$$

where $D = \tanh(rT/2)$, $t_0 = (t_1 + t_2)/2$ is the mean time of the maxima, and $T = t_1 - t_2$ is the time interval between the maxima of the pulses. Suppose that, initially, the atom is in the ground state 1 and we start the atom evolution from the initial mixing parameter $\alpha_{in}(-\infty)$ satisfying the condition $\tan(\alpha_{in}) = 0.01$, which means that essentially $C_d(-\infty)e^{-i\varphi_2} = \cos(\alpha_{in}) \approx 1$ and $C_b(-\infty)e^{i\varphi_1} = \sin(\alpha_{in}) = 10^{-2}$. We stop the atom evolution at $\tan[\alpha_{fin}(+\infty)] = 100$. So, if the final state coincides with state 2 then $C_d(+\infty)e^{-i\varphi_2} = \sin(\alpha_{fin}) \approx 1$ and $C_b(-\infty)e^{i\varphi_1} = -\cos(\alpha_{fin}) = -10^{-2}$, where the phase change of state 2 is taken into account. From Eq. (30) it follows that $\tan\alpha(\pm\infty) = (1 \pm D)/(1 \mp D)$ and at the condition imposed on $\alpha_{in}$ and $\alpha_{fin}$ we have $rT = 4.6$. Since state $b$ is strongly coupled with state $c$ [the coupling is $B(t)$], we have to keep the initial population of state $b$ as small as possible [$C_b(-\infty)$ must be close to zero]. Otherwise, the probability amplitude $C_b(-\infty)$, if not infinitely small, will be spread among the $b$ and $c$ states by the pulse train and population transfer $1 \to 2$ will be imperfect. Therefore, on the one hand, the initial value of the mixing parameter $\alpha$ must be as small as possible to have complete population transfer $1 \to 2$. For a small initial mixing angle $\alpha_{in}$, the relation between $\alpha_{in}$ and $T$ becomes simple, i.e., $\tanh(rT/2) \approx 1 - 2\alpha_{in}$. The smaller the initial value of the mixing angle $\alpha$, the larger the product $rT$ or the pulse separation $T$ is. On the other hand, if the distance between the pulses is large, the value of the coupling $B(t)$ at $t_0$ becomes small: the larger the distance, the smaller the coupling. However, the adiabatic following demands a large coupling $B$ at $t_0$. Therefore, one has to choose the optimum value of the pulse spacing satisfying two conditions simultaneously. The distance between pulses is to be as large as possible to have a small value of $\alpha_{in}$ and, at the same time, $B(t_0)$ should be kept as large as possible. Below we give some arguments on how to find this optimum value.

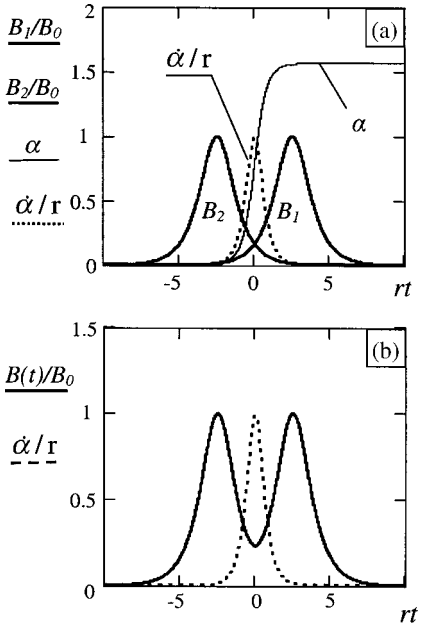


FIG. 3. (a) The pulse train with corresponding interaction parameters $B_1(t)$ and $B_2(t)$ evolving in time (bold lines). They are normalized by the maximum value $B_0$. The delay between pulses is $r\tau = 5$, $t_0 = 0$. The time is scaled in units of $r$. The time dependence of the mixing parameter $\alpha$ is shown by the thin line. The dashed line shows the dependence of the mixing parameter derivative $\dot{\alpha}$ normalized by $r$. In (b) the time dependence of the bichromatic Rabi frequency $\chi/2 = B(t)$ (solid line) and the mixing parameter derivative (dashed line) are shown for comparison.

If $rT \to 0$, then according to Eq. (30) we have $\alpha \to \pi/4$ throughout the excitation and the dark state does not change in time. It has the probability amplitude $|C_d| = \sqrt{2}/2$. State $b$, having the initial population $|C_b(-\infty)|^2 = 1/2$, is depopulated with the rate $B$ ($C_b(t) = C_b(-\infty)\cos[\theta(t)/2]$, $C_c(t) = iC_b(-\infty)\sin[\theta(t)/2]$, see the definition of $\theta(t)$ in Sec. III). For small values of $rT$, the interval of the $\alpha$ change is small. For example, if $rT = 0.5$, then $\cos(\alpha_{in}) = 0.855$, $\sin(\alpha_{in}) = 0.519$ and $\cos(\alpha_{fin}) = 0.519$, $\sin(\alpha_{fin}) = 0.855$, which corresponds to the change of $\alpha$ from $\alpha_{in} = 0.174\pi$ to $\alpha_{fin} = 0.326\pi$ during the pulse train. In this case only the fraction $(0.855)^2 = 0.731$ of the atomic population is transferred to state $|2\rangle$ if the atom adiabatically follows the dark state. Another fraction $(0.515)^2 = 0.269$ of the atomic population participates in the process of excitation and deexcitation between states $b$ and $c$. This means that the population transfer via the change of the amplitude of the dark state components is possible only if the time interval between the pulses exceeds a certain value. We choose the value $rT = 5$ since in this case the initial population of state $b$ is $4.5 \times 10^{-5}$ so that we neglect this population in our further consideration.

Figure 3(a) shows the pulse train with $rT = 5$ along with the change of the mixing parameter $\alpha$ during the excitation. On the same plot the dependence of the derivative

$$\dot{\alpha}(t) = \frac{rD\,\mathrm{sech}^2[r(t-t_0)]}{1 + D^2\tanh^2[r(t-t_0)]} \tag{31}$$

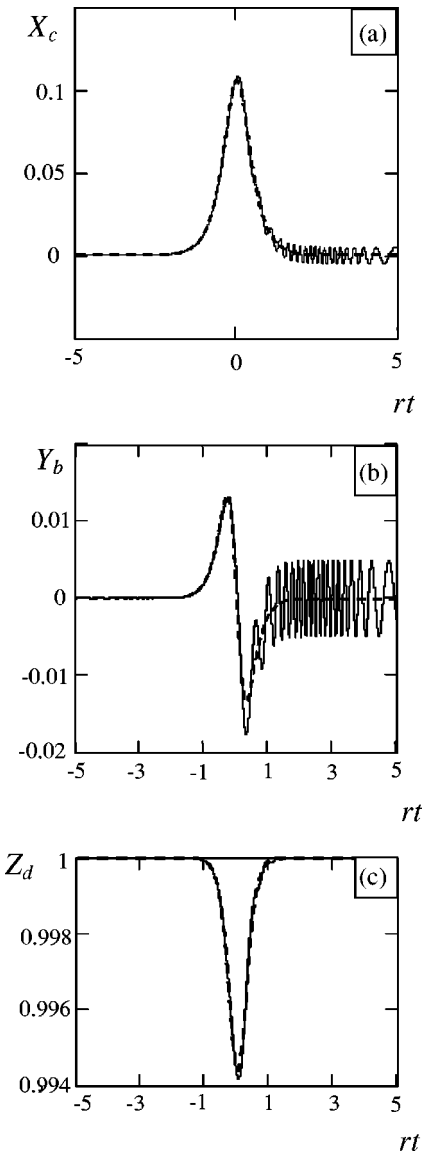


FIG. 4. (a) The evolution of the amplitudes $X_c$ [plot (a)], $Y_b$ [plot (b)], $Z_d$ [plot (c)] for a pulse train $B_1(t)$, $B_2(t)$ with the parameters $B_0=42.8r$, $t_1=2.5/r$, $t_2=-2.5/r$. Solid lines are the numerical solution of Eqs. (23)–(25). Dashed lines are analytical approximations given by the first two terms of Eqs. (36) and (37) and the first two terms in each of the parentheses of Eq. (45).

is shown. This derivative takes a maximum value $\dot{\alpha}_{\max}(t_0)=rD$ at $t=t_0$. For example, if $rT=5$, then $\dot{\alpha}_{\max}(t_0)=0.987r$. In Fig. 3(b) we compare the time evolution of the Rabi frequency $\chi_R/2=B(t)=\sqrt{B_1^2(t)+B_2^2(t)}$ with the evolution of the derivative $\dot{\alpha}(t)$.

The Rabi frequency determines the transition rate between states $b$ and $c$, whereas the derivative of the state mixing angle $\alpha$ specifies the transition rate between states $d$ and $b$ [see Eqs. (23)–(25)]. Since at $t=t_0$ the parameter $\dot{\alpha}(t)$ takes its maximum value and $B(t)$ has its minimum, the adiabatic-following condition is $B(t_0)\gg\dot{\alpha}(t_0)$ or, explicitly, $\sqrt{2}B_0\gg r\sinh(rT/2)$. Figure 4 (solid lines) shows the time dependence of the amplitudes $X_c$ [plot (a)], $Y_b$ [plot (b)], and $Z_d$ [plot (c)] obtained by the numerical solution of Eqs. (23)–(25) for the pulse train with $t_1=2.5/r$, $t_0=0$, $t_2=-2.5/r$, $T=5/r$, $B_0=42.8r$. The relation between $B_0$ and $r$ corresponds to the ratio $B(t_0)/\dot{\alpha}(t)=10$.

To estimate the probability amplitudes of the $dbc$ states during the excitation and find the borders within which the adiabatic following of the dark state takes place, we follow the theory developed by Crisp [3] for the case when the condition $B(t_0)\gg\dot{\alpha}(t)$ is well satisfied. However, in our case both $B(t)$ and $\dot{\alpha}(t)$ are time dependent, whereas Crisp considered the case when only $\dot{\alpha}(t)$ is time dependent and $B$ is constant. Therefore, we have to modify the method of Crisp.

If $B(t)\gg\dot{\alpha}(t)$ at any time, we can use the expansion in a power series of the parameter $\dot{\alpha}(t)$ for the solution of Eqs. (23)–(25). Then the first term of the expansion is found by setting $Z_d(t)=1$ in Eqs. (24) and (25) and then solving them. The solution is

$$Y_b(t)=\int_{-\infty}^{t}\cos\left[\int_{\tau}^{t}B(\tau_1)d\tau_1\right]\dot{\alpha}(\tau)d\tau, \tag{32}$$

$$X_c(t)=\int_{-\infty}^{t}\sin\left[\int_{\tau}^{t}B(\tau_1)d\tau_1\right]\dot{\alpha}(\tau)d\tau. \tag{33}$$

This is the part of the general solution that is linear in $\dot{\alpha}(t)$. $Z_d$ satisfies the equation

$$Z_d(t)=1-\int_{-\infty}^{t}\dot{\alpha}(\tau)\,Y_b(\tau)d\tau, \tag{34}$$

which is the formal solution of Eq. (23). Therefore, the change of the dark state amplitude $Z_d$ is nonlinear in $\dot{\alpha}(t)$ and can be presented in products of $\dot{\alpha}$'s. The first contribution of $\dot{\alpha}(t)$ to $Z_d$ can be found as the square of $\dot{\alpha}$, i.e., in the second term of the expansion. Substituting the corrected $Z_d$ into Eqs. (24) and (25) (instead of $Z_d=1$), one can find the next term in the expansion of $Y_b$ and $X_c$. Then the substitution of the thus found $Y_b$ into Eq. (34) gives the next term of the expansion of $Z_d$, etc. In this paper we consider only the linear corrections to $Y_b$ and $X_c$. Figures 4(a)–4(c) show the comparison of the numerical solution of Eqs. (23)–(25) with Eqs. (32)–(34). They are indistinguishable and shown by the same solid lines.

We find the adiabatic and nonadiabatic components of the analytical solution by applying two different procedures. The adiabatic components of Eqs. (32)–(33) are calculated by integrating them by parts. For example, the first step of the $X_c(t)$ calculation is

$$X_c(t)=\int_{-\infty}^{t}\frac{\dot{\alpha}(\tau)}{B(\tau)}d\left(\cos\left[\int_{\tau}^{t}B(\tau_1)d\tau_1\right]\right)$$

$$=\frac{\dot{\alpha}}{B}-\int_{-\infty}^{t}\cos\left[\int_{\tau}^{t}B(\tau_1)d\tau_1\right]\left(\frac{\dot{\alpha}}{B}\right)'_{\tau}d\tau, \tag{35}$$

where $(\dot{\alpha}/B)'_\tau$ is the derivative with respect to $\tau$. Repeating these steps several times, we obtain

$$Y_b(t)=\alpha_2-\alpha_4+\alpha_6-\alpha_8+\cdots, \tag{36}$$

$$X_c(t)=\alpha_1-\alpha_3+\alpha_5-\alpha_7+\cdots, \tag{37}$$

where $\alpha_n=\dot{\alpha}_{n-1}/B$, $\alpha_0=\alpha$, and it is assumed that $\dot{\alpha}(t)$ is a bell-shaped function with first and higher derivatives equal to zero at $t=-\infty$. To find a similar expansion of Eq. (34), we introduce the function $\Omega(t)=\int_0^t B(\tau)d\tau$. Then the equation for $Z_d(t)$ takes the form

$$Z_d(t)=1-A_c(t)-A_s(t), \tag{38}$$

with

$$A_c(t)=\int_{-\infty}^{t} d\tau_1\dot{\alpha}(\tau_1)\cos\Omega(\tau_1)\int_{-\infty}^{\tau_1} d\tau_2\dot{\alpha}(\tau_2)\cos\Omega(\tau_2), \tag{39}$$

$$A_s(t)=\int_{-\infty}^{t} d\tau_1\dot{\alpha}(\tau_1)\sin\Omega(\tau_1)\int_{-\infty}^{\tau_1} d\tau_2\dot{\alpha}(\tau_2)\sin\Omega(\tau_2). \tag{40}$$

The functions $A_c(t)$ and $A_s(t)$ are reduced to the single integrals

$$A_c(t)=\frac{1}{2}\left(\int_{-\infty}^{t} d\tau_1\dot{\alpha}(\tau_1)\cos\Omega(\tau_1)\right)^2, \tag{41}$$

$$A_s(t)=\frac{1}{2}\left(\int_{-\infty}^{t} d\tau_1\dot{\alpha}(\tau_1)\sin\Omega(\tau_1)\right)^2. \tag{42}$$

This can be done since they have the structure

$$A_{c,s}(t)=\int_{-\infty}^{t} d\tau\dot{f}_{c,s}(\tau)f_{c,s}(\tau)=\frac{1}{2}f_{c,s}^2(t), \tag{43}$$

where $f_{c,s}(\tau)$ is

$$f_{c,s}(t)=\int_{-\infty}^{t} d\tau\dot{\alpha}(\tau)\left\{\begin{matrix}\cos\Omega(\tau)\\ \sin\Omega(\tau)\end{matrix}\right\}, \tag{44}$$

and the index $c$ stands for the cosine function and index $s$ for sine. Integrating these integrals by parts, we obtain

$$Z_d(t)=1-\tfrac{1}{2}[(\alpha_1-\alpha_3+\alpha_5+\cdots)^2 +(\alpha_2-\alpha_4+\alpha_6+\cdots)^2]. \tag{45}$$

Equations (36), (37), and (45) give the probability amplitudes of the dark, bright, and common states. They coincide with those one obtains if the successive transformations $S_nS_{n-1}\cdots S_1S$ to the new set of $d_nb_nc_n$ states are performed, as was done by Fleischhauer and co-workers in Ref. [30], i.e., $|\Phi_n\rangle=S_nS_{n-1}\cdots S_1S|\Phi_0\rangle$, where $|\Phi_0\rangle=C_1|1\rangle+C_2|2\rangle+C_3|3\rangle$ is the initial state $[C_1(-\infty)=1,\ C_2(-\infty)=C_3(-\infty)=0]$. The transformation $S$ is defined in Eq. (17) and the other transformations $(S_i)$ are specified below. These transformations have a simple meaning. Since the $d$-$b$ and $b$-$c$ transitions are excited simultaneously by the $\dot{\alpha}$ and $B$ "fields," one can make an $S_1$ transformation to the new set of dark, bright, and common states, $d_1$, $b_1$, and $c_1$, where $d_1$ is a particular mixture of the former $d$ and $c$ states, $b_1$ is a state orthogonal to state $d_1$, and $c_1$ coincides with state $b$. The new mixing angle is $\alpha_1=\arctan(\dot{\alpha}/B)$. Repeating this procedure $n$ times, one can get our solution if the conditions $\arctan(\dot{\alpha}_n/B)\approx\dot{\alpha}_n/B$ and $\sqrt{\dot{\alpha}_n^2+B^2}\approx B$ are applied at each step.

Figures 4(a–c) show the comparison of the numerical solution (solid lines) with the expansions given by Eqs. (36), (37), and (45) (dashed lines). The parameters of the pulse train are specified above and they are the same as in Figs. 3(a,b). Only the first two terms of the expansions are taken into account for each plot, which is justified because $|\alpha_1|\gg|\alpha_2|\gg|\alpha_3|\gg|\alpha_4|\gg\cdots$. For the $X_c$ and $Y_b$ components, the maximum absolute values of the second terms of the expansions (i.e., the adiabatic terms) are already comparable with the amplitude of the oscillations (i.e., the nonadiabatic contribution, coming from the summation of an infinite number of the expansion terms). Of course , *nonadiabatic oscillations are not described by the main part of the adiabatic solution presented by a few leading terms of the expansion.*

Concluding this section, we refer to a particular case when $B(t)$ and $\dot{\alpha}$ have the same time dependence. This is again the case of matched pulses (see the beginning of Sec. III), however in the $dbc$ basis. Fleischhauer and co-workers, Ref. [30], classify this case as second-order matched pulses. The solution of Eqs. (23)–(25) is trivial since these equations in terms of a new variable $\zeta=\int_{-\infty}^{t}F(\tau)d\tau$ can be reduced to a set of differential equations with constant coefficients, where $F(t)=B(t)/B(t_0)=\dot{\alpha}(t)/\dot{\alpha}(t_0)$. For the first time, this analytically solvable model was considered by Vitanov and Stenholm in Ref. [43]. We would classify the case as nonadiabatic, however in the second-order $d_1b_1c_1$ basis, where the transition takes place. If the generalized pulse area is properly chosen in this basis, the population transfer between the diabatic states 1 and 2 is complete. For these particular pulse areas, there are no nonadiabatic corrections, which is typical for the resonant nonadiabatic transitions.

## V. NONADIABATIC CORRECTIONS

All adiabatic terms tend to zero at $t\to+\infty$, which secures for the three-level atom the adiabatic following of a particular state coinciding with state $d$ at $t\to+\infty$. However, as it will be shown below, if we sum all these infinitely small terms, the result will be finite. The net value of the small contributions of each adiabatic term is a nonadiabatic contribution, which specifies the excited probability amplitude left by the pulse train. To estimate this value, we rewrite the solution, Eqs. (32) and (33), as follows:

$$Y_b(t)=f_c(t)\cos\Omega(t)+f_s(t)\sin\Omega(t), \tag{46}$$

$$X_c(t)=f_c(t)\sin\Omega(t)-f_s(t)\cos\Omega(t). \tag{47}$$

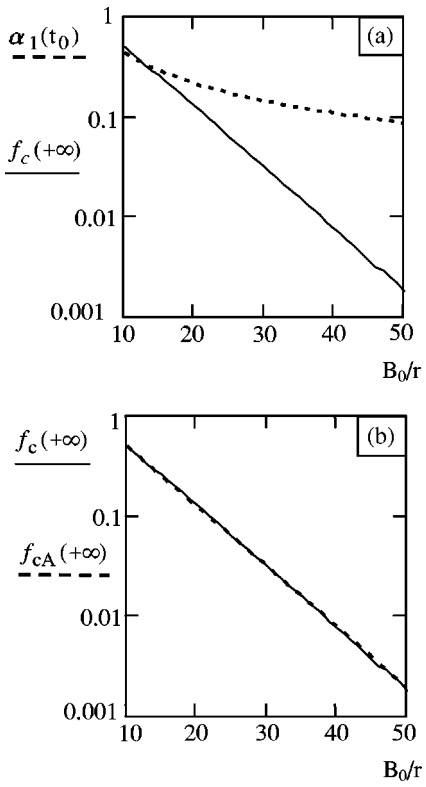


FIG. 5. (a) Comparison of the dependence of the adiabatic $\alpha_1(t_0)$ (dashed line) and nonadiabatic $f_c(+\infty)$ (solid line) parts of the analytical solution of Eqs. (23)–(25) on the maximum pulse amplitudes $B_0$. In (b) the comparison of the nonadiabatic part, numerically calculated using the actual Rabi frequency $B(t)$ (solid line) and its parabolic approximation, Eq. (53) (dashed line), are shown. $f_c(+\infty)$ is the true nonadiabatic part and $f_{cA}(+\infty)$ is an approximation.

When $t\rightarrow+\infty$, the function $f_c(t)$ tends to a finite value whereas $f_s(t)$ tends to zero since in the corresponding integrals [see Eq. (44)] $\dot{\alpha}(\tau)$ is an even function of time and $\Omega(\tau)$ is an odd function. As a result, at the end of the pulse train $Y_b(t)$ and $X_c(t)$ oscillate as $\cos\Omega(t)$ and $\sin\Omega(t)$, respectively, and they have constant amplitudes $f_c(+\infty)$. The value of $f_c(+\infty)$ defines the probability amplitude left by the pulse sequence in states $b$ and $c$.

The excitation process is adiabatic if the nonadiabatic part $f_c(+\infty)$ is small. If the nonadiabatic part becomes comparable with the main term $\alpha_1(t_0)$ of the adiabatic expansion, then we cannot describe the excitation process as adiabatic. Figure 5(a) shows the numerically found dependences of the $\alpha_1(t_0)$ term (dashed line) and the nonadiabatic contribution $f_c(+\infty)$ (solid line) on the maximum amplitude $B_0$ of the pulses for the pulse train with $Tr=5$. The adiabatic and nonadiabatic parts of the solution become comparable if $B_0<15r$.

The semilogarithmic plot of $f_c(+\infty)$ versus $B_0$, Figure 5(a), clearly demonstrates that the nonadiabatic part decreases exponentially with the increase of $B_0$. Laine and Stenholm [29] also found an exponential decrease of the nonadiabatic deviation from the ideal population transfer with increase of $B_0T$ ($B_0$ is the amplitude of each pulse at the maximum and $T$ is the interpulse distance, fixed in our case by the relation $Tr=5$, so $B_0/r$ is a variable). They followed the calculation procedure proposed by Davis and Pechukas [33,34] employing the Dykhne model [31,32]. According to Refs. [31–34] one has to find the zeros of the function $B(t)$ in a complex plane $t$ and take the one, $t_c$, that is nearest to the real axis. Then the population of the dark state after the pulse train is

$$|d(+\infty)|^2\propto\exp\left[-2\,\mathrm{Im}\int_{t_0}^{t_c}B(t)dt\right]. \tag{48}$$

We propose another calculation procedure of the nonadiabatic deviation. It will be shown that there are two nonadiabatic contributions, one coming from the Rabi frequency $B(t)$ and another from the mixing parameter derivative $\dot{\alpha}(t)$. Only the cooperative contribution of both determines the net nonadiabatic correction, while the Pechukas-Dykhne theory, taking into account only the $B(t)$ change, underestimates the nonadiabatic correction.

To show this, we express $f_c(t)$ via the Fourier transform of $\dot{\alpha}(t)$:

$$a(\omega)=\int_{-\infty}^{+\infty}d\tau\dot{\alpha}(\tau)\,e^{i\omega\tau}, \tag{49}$$

$$f_c(t)=\int_{-\infty}^{t}d\tau\cos\Omega(\tau)\frac{1}{2\pi}\int_{-\infty}^{+\infty}d\omega\,a(\omega)e^{-i\omega\tau}. \tag{50}$$

Let us consider first the case if the Raman Rabi frequency is constant, i.e., $B(t)=\beta_0=\mathrm{const}$. Then $\Omega(\tau)=\beta_0\tau$ and

$$f_c(+\infty)=\int_{-\infty}^{+\infty}d\omega\tfrac{1}{2}[\,\delta(\omega+\beta_0)+\delta(\omega-\beta_0)]a(\omega)=a(\beta_0), \tag{51}$$

where $\delta(x)$ is the Dirac delta function and $a(\omega)$ is an even function of $\omega$. The Fourier transform of the mixing parameter derivative for a secant hyperbolic pulse train can be found, for example in Ref. [44]. This function is

$$a(\omega)=\pi\frac{\sinh\left\{\dfrac{\omega}{2r}\arctan[\sinh(rT)]\right\}}{\sinh\left(\dfrac{\pi\omega}{2r}\right)}. \tag{52}$$

If we take $\beta_0=B(t_0)=\sqrt{2}B_0\,\mathrm{sech}(rT/2)$, which is the value of the Raman Rabi frequency at time $t=t_0$ when $\dot{\alpha}(t)$ takes its maximum, then for our numerical example specified above we obtain the amplitude of the nonadiabatic contribution $f_c(+\infty)=1.263\times10^{-3}$. This value is four times smaller than the amplitude of the nonadiabatic oscillations on the right tail of the functions $X_c(t)$ and $Y_b(t)$ (which is $\sim5\times10^{-3}$), shown in Figs. 4(a,b), i.e., four times smaller than the nonadiabatic contribution given by the numerical calculations of the solution of Eqs. (23)–(25).

To explain this difference and clarify the origin of the nonadiabatic contribution, we recall the interaction Hamil-

tonian in the $dbc$ basis, Eq. (21) [see also Eqs. (15) and (22)]. This Hamiltonian resembles the interaction representation Hamiltonian of the three-level system excited by two resonant ''fields'' with amplitudes $B(t)$ and $\dot{\alpha}(t)$ (see Fig. 2). Assume, first, that the couplings $B(t)$ and $\dot{\alpha}(t)$ are absent and the system is in state $d$. Then, states $d$, $b$, and $c$ can be considered as having the same energies in the interaction representation. Switching on the coupling $\dot{\alpha}(t)=a\Theta(t)$ [here $\Theta(t)$ is the Heaviside step function and $a$ is an arbitrary constant] mixes states $d$ and $b$ or in other words induces the transition $d\rightarrow b$. If the $B$ field is also present and its amplitude $\beta_0$ is constant, i.e., $B(t)=\beta_0\Theta(t)$, this $B$ field mixes states $b$ and $c$ producing a new couple of states $b'$ and $c'$, which are the states $|\overline{1}\rangle$ and $|\overline{3}\rangle$ [see Eqs. (8) and (10)]. This couple is split by the energy gap $2\beta_0=2B=2\sqrt{B_1^2+B_2^2}$ [see Eq. (6)]. This is the so-called Autler-Townes splitting [45] or quasienergy splitting [39,40]. Assume that without the $B$ field the $\dot{\alpha}$ field is in resonance with levels $d$ and $b$. The switching on of the $B$ field mixes levels $b$ and $c$, producing an additional splitting. Level $b$ moves on the frequency $B$ out of resonance with the $\dot{\alpha}$ field. If the $\dot{\alpha}$ field had a $\delta$ spectrum (in the case specified above it has only a zero-frequency component), then it would not interact with the atom. However, because of the finite spectral width of the $\dot{\alpha}$ field, its spectrum has a component with frequency $B$ on the far tail which is in resonance with the new position of level $b$. Only this spectral component excites the atom if the $B$ field is on. With increase of the $B$ field, the component of the $\dot{\alpha}$ field spectrum, which interacts with the atom, shifts further to the tail of the spectrum. If the $B$ field amplitude changes in time, several spectral components of the $\dot{\alpha}$ field interact with the atom since at each instant of time some particular spectral component is in resonance. The process of the sweeping of the splitting $B(t)$ along the tail of the $\dot{\alpha}$ field spectrum involves a broader band of the $\dot{\alpha}$ spectrum in the interaction. To find the net atom excitation in this case, we have to calculate the integral $f_c(+\infty)$ where the change of $B(t)$ is taken into account. This is done in the following two sections.

## VI. NONADIABATIC TRANSITION AS A QUANTUM JUMP: BASIC ARGUMENTS

If the Raman Rabi frequency changes during the development of the mixing parameter $\dot{\alpha}(t)$, those Rabi frequencies sweeping the frequency bandwidth of $\dot{\alpha}(t)$ contribute to the nonadiabatic corrections. To take this process into account, we have to convolute the spectral content of both the mixing parameter and the Raman Rabi frequency. In general, this calculation is nontrivial. For the case of secant hyperbolic pulses [see the time development of the pulses, the Raman Rabi frequency and the mixing parameter in Figs. 3(a,b)], it is possible to simplify the problem. Since $B(t)$ has a minimum value of $\beta_0$ at $t_0$ where $\dot{\alpha}(t)$ has its maximum, only the spectral components of $a(\omega)$ with $|\omega|\geqslant\beta_0$ contribute. Because time and frequency domains are inversely proportional, the main part of the nonadiabatic contribution appears in a short time interval around $t_0$, corresponding to the far tail of the spectral distribution $a(\omega)$. This means that the time scale of the nonadiabatic change is shorter than $1/\beta_0$, while, according to the condition imposed on the parameters, the time variation of $\dot{\alpha}(t)$ is much longer than the Rabi oscillation period $\sim 1/\beta_0$. Thus, a nonadiabatic transition takes place almost jumpwise compared to the time scale of the variation of $\dot{\alpha}(t)$. Due to this circumstance, we can simplify the calculation of the integral $f_c(+\infty)$ by expanding $B(t)$ in a power series of $t$ near $t_0$ and retaining only the first two terms of the expansion:

$$B(t)\approx\beta_0[1+g(t-t_0)^2], \tag{53}$$

where $g=r^2[3\tanh^2(rT/2)-1]/2$. We verified this approximation by comparing numerically two integrals $f_c(+\infty)$ and $f_{cA}(+\infty)$ calculated with $B(t)$ and its approximated value, Eq. (53), respectively. The comparison is shown in Fig. 5(b), where $f_{cA}(\infty)$ (dashed line) is the approximation. The dependences of both integrals on the amplitude $B_0$ are indistinguishable.

The approximation of $B(t)$ by a parabolic function helps to express $f_c(+\infty)$ via the Airy integral. Further, to simplify the notations we set $t_0=0$. Then the phase $\Omega(t)$ is

$$\Omega(t)=\beta_0\left(t+\frac{g}{3}t^3\right), \tag{54}$$

and $f_{cA}(+\infty)$ is expressed as

$$f_{cA}(+\infty)=\frac{1}{2\pi}\int_{-\infty}^{+\infty}d\tau\cos\left[\beta_0\left(\tau+\frac{g}{3}\tau^3\right)\right]\times\int_{-\infty}^{+\infty}d\omega\, a(\omega)e^{-i\omega\tau}. \tag{55}$$

Evaluating the time integral in Eq. (55), we obtain

$$f_{cA}(+\infty)=\gamma\int_{-\infty}^{+\infty}d\omega\, a(\omega)\mathrm{Ai}[\gamma(\beta_0+\omega)], \tag{56}$$

where $\mathrm{Ai}(x)$ is the Airy integral and $\gamma=1/\sqrt[3]{g\beta_0}$. We derived this equation assuming that $a(\omega)$ is an even function. The Airy integral has a different dependence for positive and negative arguments (see, for example, Ref. [46]). If $\beta_0+\omega\geqslant 0$, we have

$$\gamma\mathrm{Ai}[\gamma(\beta_0+\omega)]=\frac{1}{3}\sqrt{\frac{\beta_0+\omega}{3g\beta_0}}\left\{I_{-1/3}\left[\frac{2}{3}\sqrt{\frac{(\beta_0+\omega)^3}{g\beta_0}}\right]-I_{1/3}\left[\frac{2}{3}\sqrt{\frac{(\beta_0+\omega)^3}{g\beta_0}}\right]\right\}, \tag{57}$$

where $I_{\pm 1/3}(x)$ is the modified Bessel function of the order of $\pm\frac{1}{3}$. If the argument is negative, $\beta_0+\omega<0$, then

$$\gamma \mathrm{Ai}[\gamma(\beta_0+\omega)] = \frac{1}{3}\sqrt{\frac{|\beta_0+\omega|}{3g\beta_0}}\left\{ J_{-1/3}\left(\frac{2}{3}\sqrt{\frac{|\beta_0+\omega|^3}{g\beta_0}}\right) + J_{1/3}\left(\frac{2}{3}\sqrt{\frac{|\beta_0+\omega|^3}{g\beta_0}}\right)\right\}, \tag{58}$$

where $J_{\pm 1/3}(x)$ is the Bessel function of the order of $\pm\frac{1}{3}$. For large arguments both functions have a simple asymptotic behavior

$$\gamma \mathrm{Ai}[\gamma(\beta_0+\omega)] \approx \frac{\exp\left[-\frac{2}{3}\sqrt{\frac{(\beta_0+\omega)^3}{g\beta_0}}\right]}{2\sqrt{\pi}[g\beta_0(\beta_0+\omega)]^{1/4}}, \tag{59}$$

if $\beta_0+\omega$ is positive, and

$$\gamma \mathrm{Ai}[\gamma(\beta_0+\omega)] \approx \frac{\cos\left(\frac{2}{3}\sqrt{\frac{|\beta_0+\omega|^3}{g\beta_0}}-\frac{\pi}{4}\right)}{\sqrt{\pi}(g\beta_0|\beta_0+\omega|)^{1/4}}, \tag{60}$$

if $\beta_0+\omega$is negative. If the argument is zero, $\beta_0+\omega=0$, this function is

$$\gamma \mathrm{Ai}[\gamma(\beta_0+\omega)]|_{\omega=-\beta_0} = \frac{\Gamma\left(\frac{1}{3}\right)}{2\pi\sqrt[3]{3^{1/2}g\beta_0}}, \tag{61}$$

where $\Gamma(\frac{1}{3})\approx 2.679$ is the Gamma function.

## VII. RABI CHIRPING ONLY

If the $\dot{\alpha}$ field does not depend on time and has a value $\dot{\alpha}(t)=\dot{\alpha}(t_0)$, then $a(\omega)=2\pi\dot{\alpha}(t_0)\delta(\omega)/r$ and the main contribution to the nonadiabatic part is given by the Airy integral

$$f_{cA}(+\infty) = 2\pi\gamma \mathrm{Ai}(\gamma\beta_0)\dot{\alpha}(t_0)/r, \tag{62}$$

which has the explicit form

$$f_{cA}(+\infty) = \tanh\left(\frac{rT}{2}\right)\sqrt{\frac{\pi}{\beta_0\sqrt{g}}}\exp\left(-\frac{2}{3}\frac{\beta_0}{\sqrt{g}}\right), \tag{63}$$

expressed via approximation (59). In this section we show how the approximation, specified above, is related to the Dykhne-Pechukas model [31–34].

For large $\beta_0$, the Airy integral can be calculated by the *saddle-point methods* as shown, for example, in Ref. [47]. First, the stationary or saddle point $t_s$ is found where the phase $\Omega(t)$ becomes stationary: $\dot{\Omega}(t_s)=0$. In this point, the Raman Rabi frequency becomes zero since $\dot{\Omega}(t)=B(t)$. For the case of the positive argument of the Airy integral, the saddle point is in the complex plane and $t_s$ has only an imaginary component [$\mathrm{Re}(t_s)=0$], i.e.,

$$t_s = -\frac{i}{\sqrt{g}} = -\frac{i}{r}\sqrt{\frac{2}{3\tanh^2(rT/2)-1}}. \tag{64}$$

In fact, there are two saddle points: $t_s=\pm i/\sqrt{g}$. The negative sign is chosen to avoid exponentially increasing numbers. Then the method of stationary phase (one of the saddle-point methods) is applied. This method is applicable to integrals of the form

$$I(\beta_0) = \int_C e^{i\beta_0 f(z)}dz, \tag{65}$$

where $\beta_0$ is large and $C$ is a path in the complex plane such that the ends of the path do not contribute significantly to the integral. The idea of the method is to deform the contour $C$ so that the region of most of the contribution to $I(\beta_0)$ is compressed into as short a space as possible. This compression occurs at the saddle point.

Since the main contribution to this integral comes from the vicinity of the saddle point, one may conclude that in the adiabatic limit the atom abruptly makes a nonadiabatic transition between adiabatic states.

The Pechukas-Dykhne [33,34] recipe of the calculation of the nonadiabatic contribution is similar to the method described above since the definitions of the saddle point $t_s$ and the crossing point $t_c$, where $B(t_c)$ is zero, are the same. However, in our consideration we substituted the expression for the Raman Rabi frequency

$$B(t) = 2B_0\frac{\sqrt{1+\cosh(rT)\cosh(2rt)}}{\cosh(rT)+\cosh(2rt)}, \tag{66}$$

by the expansion near time $t_0$, Eq. (53). Therefore, we have only two saddle or crossing points, Eq. (64), whereas Eq. (66) has an infinite number of crossing points in the complex plane. According to Pechukas, one has to take the crossing point that is nearest to the real axis. For the secant hyperbolic pulse train, this point, as shown by Stenholm [29], has only an imaginary part $\mathrm{Im}(t_c)$, i.e.,

$$t_c = \frac{i}{r}\tan^{-1}\left[\coth\left(\frac{rT}{2}\right)\right]. \tag{67}$$

Reformulating the Dykhne approach [31,32] we conclude that if there are no spectral components of $a(\omega)$ matching the frequency gap between the quasienergy levels split by the $B$ field, the $\dot{\alpha}$ field comes to resonance with the $d$-$c$ transition at the imaginary time $t_c$ when $B$ is zero.

This approach disregards the spectral content of $\dot{\alpha}(t)$. If we take $\dot{\alpha}(t)=\dot{\alpha}(t_0)$ throughout the excitation, this method gives also an underestimated value of the nonadiabatic contribution. For our numerical example, Eq. (63) gives $f_{cA}(+\infty)=7.131\times 10^{-4}$, which is seven times smaller than the value of the nonadiabatic contribution given by the numerical calculation of the Schrödinger Equations (23)–(25). Figure 6(a) shows the comparison of the numerically calculated nonadiabatic component $f_c(+\infty)$ (solid line), Eq. (44), with that calculated for the case if the time dependence of the

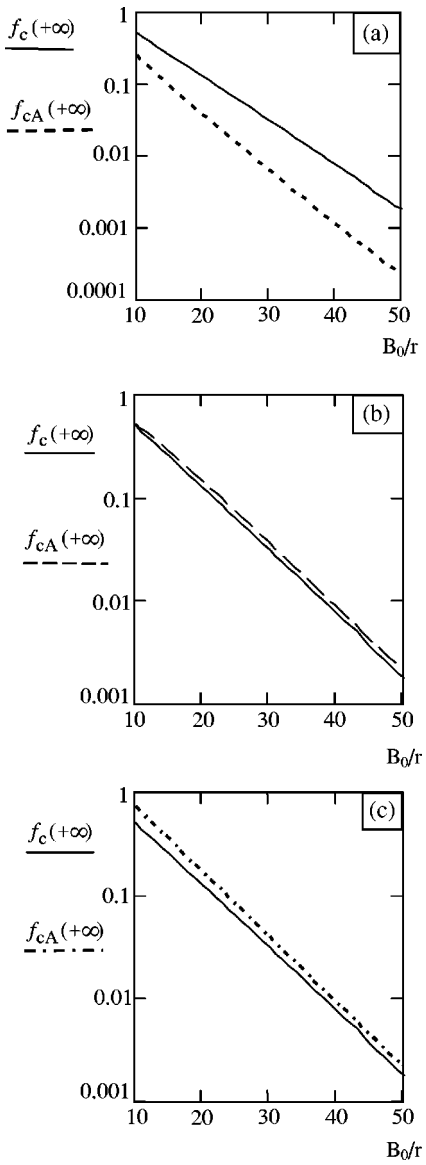


FIG. 6. (a) Comparison of the dependencies of the nonadiabatic contributions $f_c(+\infty)$ (solid line) and $f_{cA}(+\infty)$ (dashed line) vs the pulse amplitude $B_0$. The first is calculated with and the second without taking into account the time dependence of the mixing parameter derivative $\dot{\alpha}(t)$. (b) The plots of the true, $f_c(+\infty)$, and the approximate, $f_{cA}(+\infty)$, nonadiabatic contributions vs $B_0$, where $f_{cA}(+\infty)$ (long dashed line) is calculated taking into account the time dependence of $\dot{\alpha}(t)$ using the approximation described in the text. (c) The same plots as in (b), except $f_{cA}(+\infty)$ (dot dashed line), where the correction factor $K$ is dropped (see the text).

$\dot{\alpha}(t)$ field is neglected (dashed line). The latter is given by Eq. (63). The plots obviously demonstrate that this approximation underestimates the nonadiabatic contribution.

## VIII. COOPERATIVE CONTRIBUTION OF RABI CHIRPING AND THE TIME-DEPENDENT COUPLING, THE APPLICATION TO STIRAP BY SECANT HYPERBOLIC PULSES

In previous sections we showed that the contribution to the nonadiabatic corrections of the Rabi frequency chirping or the time dependence of the $\dot{\alpha}(t)$ field, being taken into account separately, was not enough to have the right nonadiabatic correction for STIRAP induced by secant hyperbolic pulses. Only both processes taken together, i.e., the Rabi frequency $B(t)$ chirping and the participation of all spectral components $a(\omega)$ of the $\dot{\alpha}(t)$ field engaged by this chirping to excite the atom, give the right value of the nonadiabatic component. This value is given by Eq. (56). To calculate analytically the convolution integral of the two spectra, $a(\omega)$ and the Airy integral describing the process of the Rabi frequency sweeping, we make two approximations. First, we take the approximation of the Airy integral, given by Eq. (59) in the frequency domain $\omega \geqslant -\beta_0$. This gives a small overestimation of the integrand near $-\beta_0$. For this reason, we start the integration from this value, not from $-\infty$. The oscillating part of the Airy integral for $\omega < -\beta_0$ gives a much smaller contribution than the main part, which is located between $-\beta_0$ and zero, $(-\beta_0,0)$. So, neglecting the part $(-\infty,-\beta_0)$, we compensate the overestimation near $-\beta_0$. Second, we approximate the spectrum $a(\omega)$ in the domain $(-\beta_0,0)$ by

$$a(\omega)=\pi\exp(-R|\omega|), \tag{68}$$

where $R=(\pi-\arctan[\sinh(rT)])/2r\approx\pi/4r$. This approximation also gives a slight overestimation of the integrand near $\omega\sim 0$. To compensate this, we stop the integration at $\omega=0$. The integrand has a maximum between $\omega=-\beta_0$ and $\omega=0$. To calculate the contribution of this part, we use the modified method of the saddle-point method. Usually, in the method of the saddle point, the integration near the point is extended to $\pm\infty$. In our case, to avoid the overestimation of the integrand we limit the integration by finite boundaries. The calculation of these boundaries for the deformed integration contour $C$ is simple because the deformed $C$ stays on the real axis. The result of the integration is

$$f_{cA}(+\infty)=\pi K\exp\left[-\beta_0 R\left(1-\frac{1}{3}gR^2\right)\right], \tag{69}$$

where $K$ is a correction factor, which takes into account the finite integration boundaries to avoid the overestimation of the integral. Explicitly, we have

$$K=\frac{1}{2}[\mathrm{erf}(h_{\max})+\mathrm{erf}(h_{\min})], \tag{70}$$

$$h_{\max}=\sqrt{\beta_0\left[\frac{2}{3\sqrt{g}}-\left(\frac{2}{3}\right)^{4/3}R+\frac{1}{3}R^3g\right]}, \tag{71}$$

$$h_{\min}=\sqrt{\frac{\beta_0 gR^3}{3}}, \tag{72}$$

and $\mathrm{erf}(x)$ is the error function. Figure 6(b) shows the comparison of the true nonadiabatic contribution $f_c(+\infty)$ (solid line) with our approximate calculation of $f_{cA}(+\infty)$, given by Eq. (69) (dashed line). Figure 6(c) compares the same dependencies if the correction factor is $K=1$ (dash dotted line).

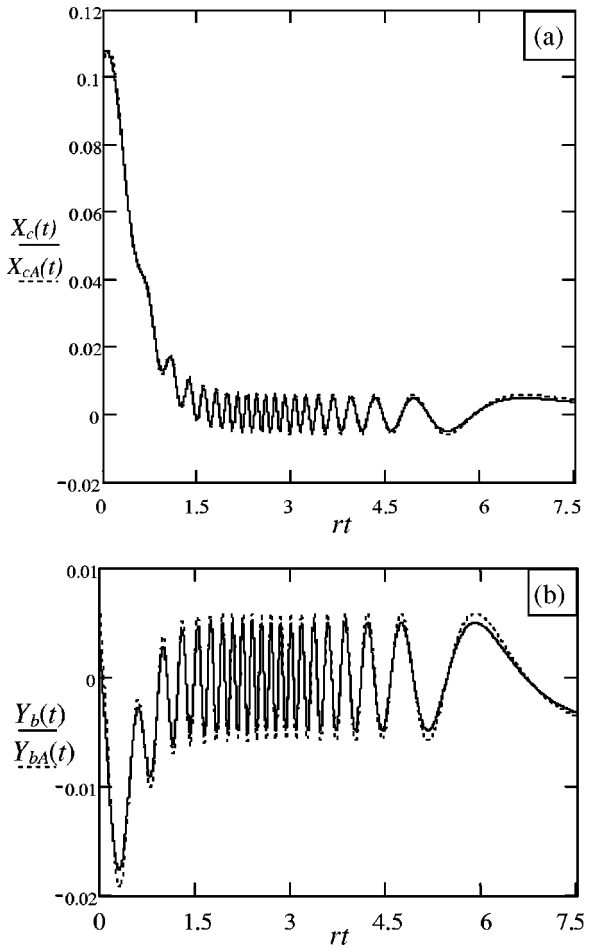


FIG. 7. Numerical solution of the Schrödinger equation (solid lines) for the amplitudes $X_c(t)$ [plot (a)], $Y_b(t)$ [plot (b)] and the approximation given by Eqs. (73) and (74) (dashed lines) for the amplitudes $X_{cA}(t)$ [plot (a)], $Y_{bA}(t)$ [plot (b)].

For our numerical example specified above, the approximated value of the nonadiabatic contribution is $f_{cA}(+\infty) = 5.822 \times 10^{-3}$. As was discussed above, this contribution appears in a very short time interval around $t_0$. Therefore, we can approximate the solution of the Schrödinger equations (23)–(25) by

$$Y_{bA}(t) \approx \alpha_2 - \alpha_4 + \Theta(t-t_0) f_{cA}(+\infty) \cos \Omega(t), \quad (73)$$

$$X_{cA}(t) \approx \alpha_1 - \alpha_3 + \Theta(t-t_0) f_{cA}(+\infty) \sin \Omega(t), \quad (74)$$

where the index $A$ stands for the approximation, $\Theta(t-t_0)$ is the Heaviside step function, $\Omega(t) = \int_0^t B(\tau) d\tau$, and $B$ has its exact value [not approximation (53)]. Figures 7(a,b) show the comparison of the numerically found solutions of the Schrödinger equation (solid lines) with approximations (73) and (74) (dashed lines). The fit of the solutions is striking. This means that the nonadiabatic contribution really appears in a quite short time range around $t_0$.

## IX. CONCLUSION

The introduction of the basis of the dark and bright states facilitates the understanding of the physical processes in the three-level atom excited by a bichromatic field. The dynamic evolution of the atom among the dark, bright, and common states is as simple as the dynamics of the two-level atom excited by one field with Rabi frequency $B$. This is because the evolution of the three-level atom can be effectively reduced to the evolution between two states, i.e., the bright and common states. The reduction of the three-level model to the two-level one allows also the application of the Bloch-vector model and Bloch equations for the treatment of the three-level atom excitation by the bichromatic field.

This quite simple algebra is applicable for the case of matched pulses. If the pulses do not match in shape and have different time dependencies, one can also reduce the consideration to the Bloch-vector model since there is a similarity between the Schrödinger equations for the probability amplitudes of the dark, bright, and common states and the Bloch equation for an effective two-level system. The effective detuning of the two-level system from resonance is $B(t)$ and the Rabi frequency is $\dot{\alpha}(t)$, which is the derivative of the mixing angle in the dark state development in states of the reciprocal three-level system. This similarity allows a simple interpretation of the physical processes in the three-level system in case of adiabatic following of the dark state by use of the Crisp theory [3].

We developed an approximation describing the adiabatic interaction of the three-level atom with two resonant pulses. The method of estimation of the nonadiabatic correction is presented. It is applied to the case of two secant hyperbolic pulses. The adiabatic part of the solution describes the excitation and deexcitation processes of the three-level atom. The time dependence of the adiabatic part is smooth and follows the derivatives of the mixing angle $\alpha(t)$. Both parts, excitation and deexcitation, are symmetric in time with respect to $t=0$ where $\dot{\alpha}(t)$ takes its maximum and they exactly compensate each other. In this respect the adiabatic following resembles the solitonlike interaction with the field. The nonadiabatic part appears in a short time interval in the vicinity of the maximum of the mixing parameter $\dot{\alpha}(t)$. It contains the information about the excitation left in the atom by the pulses because of the imperfect following of the dark state. Since this excitation lasts only a short time, we consider the nonadiabatic process as a transition between the ground and excited states, which takes place like a jump. The origin of the transition has a simple interpretation. The parameter $B$ defines the coupling strength of the bright ($b$) and common ($c$) states of the three-level system in the $dbc$ basis. The parameter $\dot{\alpha}(t)$ defines the coupling strength of the bright and dark ($d$) states. It is assumed that, initially, the system is in the dark state and any time we have $B \gg \dot{\alpha}(t)$. The $B$ coupling moves the bright state from the resonance with the $\dot{\alpha}(t)$ coupling to the value determined by the frequency $B$. If the spectral content of the $\dot{\alpha}(t)$ coupling has a component with frequency $B$, the nonadiabatic transition takes place. If $B$ changes in time, several spectral components of the $\dot{\alpha}(t)$

coupling contribute to the transition. Our results are compared with those of Laine-Stenholm [29] and Fleischhauer *et al*. [30].

We found the boundary limiting the applicability of the adiabatic following consideration. The adiabatic-following is violated if the nonadiabatic contribution becomes comparable with the first term of the adiabatic expansion [see Sec. V and Fig. 5(a)]. The presented theory, as in the theories developed in Refs. [29,30], disregards the relaxation processes, which is justified if the relaxation time is much longer than the time scale of the STIRAP pulse sequence and the period of the Rabi oscillations during the population transfer. If the relaxation time (e.g., the lifetime of the excited state 3) is comparable or much shorter than the abovementioned parameters, then one has to pursue a different approach.

The simplified algebra developed in this paper could be useful for the description of the atom state manipulation by coherent fields.

## ACKNOWLEDGMENTS

This work was supported by the Fonds voor Wetenschappelijk Onderzoek Vlaanderen, the UIAP program of the Belgian government, ISTC (Grant No. 2121), and the Russian Foundation for Basic Research.

[1] See, for example, the review by K. Bergmann, H. Theuer, and B.W. Shore, Rev. Mod. Phys. **70**, 1003 (1998).
[2] R.N. Shakhmuratov, J. Odeurs, R. Coussement, P. Mégret, G. Kozyreff, and P. Mandel, Phys. Rev. Lett. **87**, 153601 (2001).
[3] M.D. Crisp, Phys. Rev. A **8**, 2128 (1973).
[4] L.V. Keldysh, Zh. Eksp. Teor. Fiz. **47**, 1945 (1964) [JETP **20**, 1307 (1965).
[5] A.M. Perelomov V.S. Popov, and V.S. Terentyev, Zh. Eksp. Teor. Fiz. **50**, 1393 (1966) [JETP **23**, 924 (1966); **51**, 309 (1966) [**24**, 207 (1967)].
[6] A.I. Nikishov and V.I. Ritus, Zh. Eksp. Teor. Fiz. **50**, 255 (1966) [JETP **23**, 168 (1966); **52**, 223 (1967) [**25**, 145 (1967)].
[7] Yu.A. Bychkov, and A.M. Dykhne, Zh. Eksp. Teor. Fiz. **58**, 1734 (1970) [JETP **31**, 928 (1970)].
[8] A.H. Zewail, Sci. Am. **263(12)**, 40 (1990); J. Phys. Chem. **97**, 12427 (1993).
[9] G. Beddard, Rep. Prog. Phys. **56**, 63 (1993).
[10] B.M. Garraway and K.-A. Suominen, Rep. Prog. Phys. **58**, 365 (1995).
[11] L.D. Landau, Phys. Z. Sowjetunion **1**, 89 (1932); **2**, 46 (1932).
[12] C. Zener, Proc. R. Soc. London, Ser. A **137**, 696 (1932).
[13] N. Rosen and C. Zener, Phys. Rev. **40**, 502 (1932).
[14] E.C. Stueckelberg, Helv. Phys. Acta **5**, 369 (1932).
[15] J.B. Delos, and W.R. Thorson, Phys. Rev. A **6**, 720 (1972); **6**, 728 (1972).
[16] G.V. Dubrovskiy and I. Fisher-Hjalmars, J. Phys. B **7**, 892 (1974).
[17] D.S.F. Crothers, Adv. Phys. **20**, 86 (1971); **20**, 405 (1971); J. Phys. A **5**, 1680 (1972); J. Phys. B **9**, 442 (1975); **9**, 635 (1976).
[18] M.S. Child, Molec. Phys. **31**, **4**, 1031 (1976).
[19] J. Oreg, F.T. Hioe, and J.H. Eberly, Phys. Rev. A **29**, 690 (1984).
[20] F.T. Hioe, and J.H. Eberly, Phys. Rev. Lett. **47**, 838 (1981).
[21] F.T. Hioe, Phys. Rev. A **28**, 879 (1983); **29**, 3434 (1984); **30**, 3097 (1984).
[22] J.R. Kuklinsky, U. Gaubatz, F.T. Hioe, and K. Bergmann, Phys. Rev. A **40**, 6741 (1989).
[23] F.T. Hioe and C.E. Carroll, Phys. Rev. A **37**, 3000 (1988).
[24] C.E. Carroll and F.T. Hioe, Phys. Rev. A **42**, 1522 (1990).
[25] E. Arimondo, *Coherent Population Trapping in Laser Spectroscopy*, edited by E. Wolf, Progress in Optics Vol. 35 (Elsevier Science, Amsterdam, 1996), pp. 257–354.
[26] E. Arimondo and G. Orriols, Nuovo Cimento Lett. **17**, 333 (1976).
[27] H.R. Gray, R.M. Whitley, and C.R. Stroud, Jr., Opt. Lett. **3**, 218 (1978).
[28] G. Orriols, Nuovo Cimento B **53**, 1 (1979).
[29] T.A. Laine and S. Stenholm, Phys. Rev. A **53**, 2501 (1996).
[30] M. Fleischhauer, R. Unanyan, B.W. Shore, and K. Bergmann, Phys. Rev. A **59**, 3751 (1999).
[31] A.M. Dykhne, Z. Eksp. Teor. Fiz. **38**, 570 (1960) [Sov. Phys. JETP **11**, 411 (1960)]; **41**, 1324 (1961) [**14**, 941 (1962)].
[32] A.M. Dykhne and A.V. Chaplik, Zh. Eksp. Teor. Fiz. **43**, 889 (1962) [JETP **16,** 631 (1963)].
[33] J.P. Davis and P. Pechukas, J. Chem. Phys. **64**, 3129 (1976).
[34] J.-T. Hwang and P. Pechukas, J. Chem. Phys. **67**, 4640 (1977).
[35] M.V. Berry, Proc. R. Soc. London, Ser. A **414**, 31 (1987); **429**, 61 (1990).
[36] R. Lim and M.V. Berry, J. Phys. A **24**, 3255 (1991).
[37] M.V. Berry and R. Lim, J. Phys. A **26**, 4737 (1993).
[38] R. Lim, J. Phys. A **26**, 7615 (1993).
[39] Ya.B. Zeldovich, Usp. Fiz. Nauk **110**, 139 (1973) [Sov. Phys. Usp. **16**, 427 (1973)].
[40] A.R. Kessel and R.N. Shakhmuratov, Physica B & C **92**, 132 (1977).
[41] S.E. Harris, Phys. Rev. Lett. **70**, 552 (1993); **72**, 52 (1994).
[42] S.E. Harris and Z.-F. Luo, Phys. Rev. A **52**, R928 (1995).
[43] N.V. Vitanov and S. Stenholm, Phys. Rev. A **55**, 648 (1997).
[44] A. Erdélyi, W. Magnus, F. Oberhettinger, F.G. Tricomi, and H. Bateman, in *Tables of Integral Transforms*, edited by A. Erdélyi (McGraw-Hill, New York, 1954), Vol. I, p. 30.
[45] S. Autler and C.H. Townes, Phys. Rev. **100**, 703 (1955).
[46] *Handbook of Mathematical Functions*, edited by M. Abramowitz and I.A. Stegun (Dover, New York, 1965).
[47] J. Mathews and R.L. Walker, *Mathematical Methods of Physics* (Benjamin, New York, 1965), p. 111.